

## DESIGN AND SIMULATION OF DIATOMACEOUS NANO-FILTER USING TITANIUM OXIDE NANOPARTICLES (TiO<sub>2</sub>-NPs) AND FRUSTULE NANOSTRUCTURES: BASED ON FLOW DYNAMICS MODELING IN PILOT-SCALE

M. SAADATI<sup>a</sup>, S. IMANI<sup>b,f\*</sup>, E. N. WARZAGHANY<sup>c</sup>,  
M. A. DEHGHANI<sup>d</sup>, S. HAJIHOSSEINI<sup>e</sup>, M. MOSTAGHACI<sup>e</sup>, J. J. FU<sup>f</sup>

<sup>a</sup>*Applied Biotechnology and Environmental Research Center, Baqiyatallah Medical Science University (BMSU), Tehran, Iran.*

<sup>b</sup>*Chemical Injuries Research Center, Baqiyatallah Medical Sciences University (BMSU), Tehran, Iran.*

<sup>c</sup>*Department of Aerospace, Faculty of Mechanics, Imam Hossein University, Tehran, Iran.*

<sup>d</sup>*Department of Mechanical, Bu-Ali Sina University, Hamadan, Iran.*

<sup>e</sup>*Industrial Diseases Research Center, Center of Excellence for Occupational Medicine, Shahid Sadoughi University of Medical Sciences, Yazd, Iran.*

<sup>f</sup>*Key Laboratory of Epigenetics and Oncology, Research Center for Preclinical Medicine, Southwest Medical University, Luzhou, Sichuan 646000, China.*

This study aimed to design the nanofilter using photocatalytic TiO<sub>2</sub>-NPs on the siliceous frustules of diatom's composite under UV-light irradiation. TiO<sub>2</sub>-NPs synthesized by sol-gel method, and were characterized by XRD and TEM methods. The diatomaceous composite were described by SEM and FPXRF. Darcy and CFD equations were used to measure the initial length, filter mass flow rate, area-weighted average of pressure and velocity cantors. The quality and kinetic of nanofilter were measured by assessing of common bacterial coliforms. More than 85% of diatomaceous soil was SiO<sub>2</sub> and crystal size of TiO<sub>2</sub>-NPs/SiO<sub>2</sub> composite was 25 nm. The mass flow rate and area-weighted average of velocity cantors were increased to 1.07 (g/s) and 0.289 (m/s), respectively. The sporicidal and total coliform removal capability of nanofilter were 80.8% and 85.8% of filtering capability, respectively. The nanofilter capacity has been statistically declining for 3<sup>th</sup> filtering in compared with 1<sup>th</sup> and 2<sup>th</sup> filtration (-6% efficiency, P=0.033). Instead, bactericidal capabilities were inversely correlated by filtering time (R=-0.81, P=0.93). The TiO<sub>2</sub>-NPs/SiO<sub>2</sub> composite is appropriate for filtering of water coliforms.

(Received March 1, 2016; Accepted April 27, 2016)

**Keywords:** Diatoms - Siliceous frustules - Filtering - Titanium oxide nanoparticles - Coliform.

### 1. Introduction

One of the main concerns of human societies in the past two decades has been shortage of drinking water (Baron et al., 2015, Kim et al., 2016). According to people action international (PAI) estimate, more seriously over 2.8 billion people in 48 countries will face water stress by 2025 (PAI, 1997). Population growth, extended droughts, increasing groundwater exploitation, unmitigated flooding and industrialization increasing are considered as a main reasons of water resource shortage (Keeley et al., 2016).

\* Corresponding author: [saberimani@swmu.edu.cn](mailto:saberimani@swmu.edu.cn)

Filtration is one of the water portable ways has been used long ago (Bilad et al., 2013). Filtering methods that purifying water in a quite safe manner, are highly regarded. Among the different methods of filtering water, the usage of photocatalytic nanoparticles (NPs) has boomed (Funayama et al., 1987). The mixture of NPs, especially metal oxide NPs (i.e., filler) in a polymer material (i.e., matrix) and a thin-film nanocomposite (TFN), the formation of a thin-film layer with fillers on a porous matrix are the two types of nanotechnology enhanced water filtration materials (Khan et al., 2014). This technology as a greatest achievements of nanotechnology, served humanity by controlling disease-causing agents in water.

Various NPs can be applied as a filter of nanocomposite membranes (Gao et al., 2015, Liu et al., 2015). Among the various studied nanomaterials, titanium oxide nanoparticles ( $\text{TiO}_2$ -NPs) have received a great deal of attention. The  $\text{TiO}_2$ -NPs have excellent mechanical, photocatalytic, thermal and partial antibacterial properties (Li et al., 2015b, Li et al., 2014, Oza et al., 2013). The application of  $\text{TiO}_2$ -NPs as water nanofilter is assisted by photocatalysis. The stimulated  $\text{TiO}_2$ -NPs under solar light illumination have been shown to be potentially advantageous and useful in filtrations (Mor et al., 2005). It's well established that the  $\text{TiO}_2$ -NPs arrays of variable wall thickness are used to photo cleave water under ultraviolet irradiation. In addition, wall thickness and length of the  $\text{TiO}_2$ -NPs can be controlled via anodization bath temperature (Mor et al., 2005, Zhang et al., 2006, Wang et al., 2006).

On the other hand, researchers have tried to increase NPs-based filter capacity with coupled in biologicals substance. Due to properties and their ingredients, the algae are a good candidate for use as water filters (Thakkar et al., 2015, Wang et al., 2012, Delalat et al., 2015). Diatoms are known as microscopic, unicellular algae which possess intricate exoskeletons made of amorphous silica (renowned frustules) (Chandrasekaran et al., 2015, Scherer et al., 2005). The frustules are natural hierarchical porous silica structure. In recent decades, researchers have showed the design and produce specific frustule morphologies that have potential applications. The silica is the main material of exoskeleton of a diatoms that can be regarded as a photonic crystal slab waveguide with moderate refractive-index contrast. It's possible to design and produce of photo catalysts that mimic the architectures of diatoms with their light-harvesting properties and are able to operate effectively under UV- light irradiation are greatly appealing in water filtering (Sakai et al., 2013).

In this study, we propose the novel diatomaceous photo catalysis-assisted water nanofilter that design based photocatalytic properties of  $\text{TiO}_2$ -NPs on the frustule nanostructures. According our mind, the diatoms played the roles both bio templates and resources of silica in the synthetic nanofilter. The combination of the diatom structure and the existence of the  $\text{TiO}_2$ -NPs in the as-prepared  $\text{TiO}_2$ -NPs/ $\text{SiO}_2$  composite render it as improved photocatalytic performance under UV-light irradiation.

## **2. Materials and methods**

### **2.1 Materials**

All materials and chemical reagent such as Ethanol (puriss p.a. absolute 99.8%), titanium isopropoxide (IV) salt (TTIP) (98% pure), and titanium (IV) n-butoxide (TNB,  $\text{C}_{16}\text{H}_{36}\text{O}_4\text{Ti}$ , purum N 97%) were purchased from Sigma-Aldrich Co. (St. Louis, MO, USA). All evaluation salts dissolved in two ionizing water. Diatomaceous soil was purchased from Ceca Co. (Clarcel®, Paris, French). The growing and maintaining the microbiological cultures media such as, nutrient agar/broth, Luria-Bertani (LB) agar, Salmonella Shigella (SS) agar, Muler-Hinton agar, tryptone, yeast extract of Bacto TM, Cook Meat Media (CMM), and etc. were purchased from Himedia (Mumbai, India) and Merck (E. Merck Co; Darmstadt, Germany). All reagents were of analytical grade and used without further purification.

### **2.2 Bactericidal strains and culture conditions**

Species considered of *Escherichia coli* (*E. coli*) (ATCC 25922), *Vibrio cholera* (*V. cholera*) (ATCC 14033), *Shigella dysenteriae* (*S. dysenteriae*) (ATCC 13313) were used during

the present experiment. All strains were obtained from the Iranian Research Organization for Science and Technology (IROST). Only spore of *Clostridium botulinum type E* (*C. botulinum*) was prepared by Environmental Science Research Center of *Imam Hussein University* (IHU). Aqueous solutions and bacterial suspensions were prepared using distilled deionized sterile water.

All samples were inoculated in a shaker-incubator at 36 °C overnight. After the growth of the species, optical density (ODs) of all samples were measured. The species of *C. botulinum* cutlers and spores purifications methods described previously (Ali mohammad Zand et al., 2012). Briefly, bacteria were cultured in CMM for 72 h, at 32 °C in aerobic jar containing 15% nitrogen and carbon dioxide gas. Then, spores of *C. botulinum* were purified by Peterson method according in our previous published articles (Ali mohammad Zand et al., 2012). The composition and concentrations of microbial that injected into the deigned nanofilter as an initial injection volume were sorted in Table 2.

### 2.3 Syntheses of titanium oxide nanoparticles

TiO<sub>2</sub>-NPs were synthesized using Sol-gel method. According this method, TTIP was dissolved in ethanol, then in deionized water with ratio of 1:4. The nitric acid was used for inhibiting the hydrolysis process. Sol solution was obtained after 30 min, other than the gel was placed for 24 h for drying in calcination temperature (120 °C for 2 h) to evaporate water and organic material. Finally, TiO<sub>2</sub>-NPs were obtained from gel after placed at 450 °C for 2 h. The anatase phase of TiO<sub>2</sub>-NPs could be formed after incubation for 2 h at 450 °C (for calcination in the drying gel phase). Physical characteristics of the synthesized nanocomposites were evaluated, by X-ray diffraction (XRD) (D 8 Advance, Bruker, Germany) of Cu Ka radiation ( $k = 0.15406$  nm) with the scanning rate of 0.01/step and for 2 h, ranging from 5 to 80. In addition, transmission electron microscopy (TEM) micrographs were taken using Hitachi-HU-12A TEM. A drop of this diluted solution was added to fomvar/carbon-coated grids (400 meshes); after drying, studied under the TEM (Brazilian Synchrotron Light Laboratory, Sao Paulo, Brazil), operating at 200 kV.

### 2.4 Preparation of diatomaceous soil

Confirmatory chemical analysis of diatomaceous soil was carried out by field portable X-ray fluorescence spectrometer (FPXRF) (X DELTA-50 FPXRF, Olympus), to measure soil composition. The measurement time was 120 s per point and the soil mode calibration and software using compton normalization provided with the instrument by the manufacturer was used for quantification. Certified soil standards (NIST 2710a and 2711a) were analyzed every 20 measurements to check the instrument performance. Each time, it was verified that the target elements were within 20% of the certified concentrations. Typically, the measurements would be within more than 80% of the certified values for clean Silica (Si) and silicon dioxide (SiO<sub>2</sub>). For remove extras minerals, the diatomaceous soil was washed with deionized water three times. After drying in the oven, 1 gr of soli was crushed in diamond grinding polishing machine (Inland, NE, USA). Then, the morphologies of diatomaceous soil particles were characterized using DSM 960 A, Zeiss scanning electron microscope (SEM) (German Electronic Company, German).

### 2.5 Modeling and simulation of the nanofilter

In this modeling, the filter mass flow rate, area-weighted average of pressure and velocity were evaluated by Darcy equation. The pressure, original length, and the overall structure of the nanofilter were simulated in 30 mm diameter of cylindrical model of nanofilter (30×100 mm) under Solidox and Fluent software. In these models, the ground pressure was considered as a base pressure in the height of half a meter from the surface of the nanofilter base. However, the all simulation results were confirmed by computational fluid dynamics (CFD) analysis in two and three-dimensional.

### 2.6 Preparation of nanofilter bed

According to the optical catalytic properties of TiO<sub>2</sub>-NPs, 10% (v/v) of diatomaceous soil and TiO<sub>2</sub>-NPs were mixed in the 30 mm cylindrical model of deigned nanofilter. To stimulate of photoactinic properties of TiO<sub>2</sub>-NPs were used the UV Lamp (250 to 270 nm wavelength). The voltage required to activate the UV lamp, was 6 V so, AC power is converted to 6 V using an

adapter. For each studied species, 5 ml of pathogenic soup was injected to nanofilter and the maximum bactericidal activity was reported according the colony-forming unit (CFU) in milliliters (CFU/ml) of effluent. Also, the efficiency of the filter was evaluated by 3 times filtration with an interval of 24 h.

### 2.7 Antibacterial evaluations

To evaluate the performance of the deigned nanofilter, a combination soup of pathogens were prepared. For this reason, 100  $\mu$ L of each bacterial species were inoculated in sterile buffered saline. Also 100  $\mu$ L of purified spores were added to the soup and then 0.5 ml of this soup was injected to nanofilter. The filtration rate and efficiency of the nanofilter were investigated based on the amount of the CFU/ml. In this investigations, we consider the total coliform a 10 ml of each studied strains.

### 2.8 Statistical methods

All statistical analyses were performed using SPSS software version 21.0 (Chicago, Illinois, USA). Totally tests were repeated three times or more. Data were presented as means  $\pm$  Std. Deviation (SD) or median (range). For all tests, two-sided p values less than 0.05 were considered statistically significant. All charts were designed by Prism 5.0 (Graph Pad, La Jolla, CA, USA).

## 3. Results

### 3.1 The characteristics of the diatomaceous soil

The size distribution of the diatomaceous soil particles were shown in the Fig. 1. This figure shown that main diatomaceous soil particles sizes are in the range of 10-70  $\mu$ m. Expectedly, the FPXRF results determined that more than 85% of the studied diatomaceous soil was composed of SiO<sub>2</sub>. In this regard, Al<sub>2</sub>O<sub>3</sub> and Fe<sub>2</sub>O<sub>3</sub> were meaningfully higher in composition of diatomaceous soil(3.4% and 2.3%, respectively). Furthermore, the diatomaceous soil particles were compared before and after diamond grinding polishing and washing in the Fig. 2. The SEM images of diatomaceous soil particles show that before crushing particles size was  $\geq$ 120 nm (Fig. 2a), but after polishing transformed to  $\leq$ 80 nm NPs(Fig. 2b).

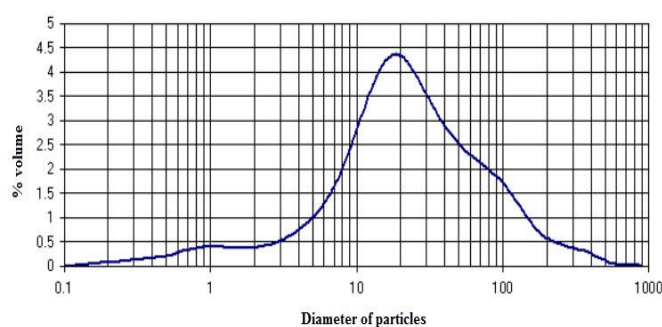


Fig. 1. Size distribution of the diatomaceous soil particles.

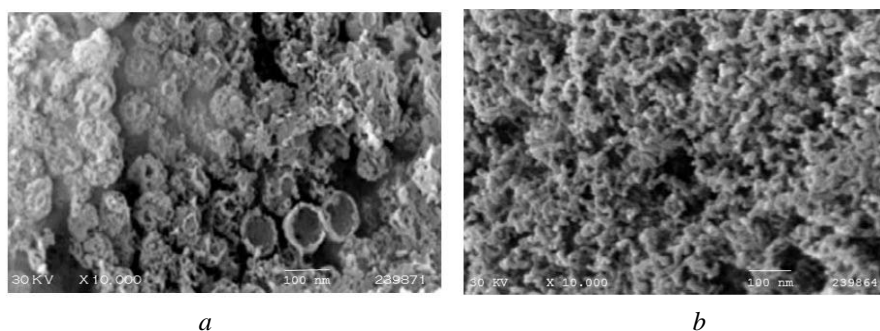


Fig. 2. SEM images of diatomaceous soil particles before (a) and after (b) the process of diamond grinding polishing and washing. SEM, scanning electron microscopy.

### 3.2 The characterization of titanium oxide nanoparticles

The Fig. 3 showed the results of the characterization of synthesized  $\text{TiO}_2$ -NPs. The XRD diffraction patterns of the crystal structure of synthesized  $\text{TiO}_2$ -NPs measured for corresponding samples were investigated. According Scherrer formula, the XRD patterns stabled the size of NPs demonstrated the size NPs were 20 nm (Fig. 3a). Also, the TEM image of the crystal structure of  $\text{TiO}_2$ -NPs demonstrated that the average size of NPs were nearly 23 nm (Fig. 3b).

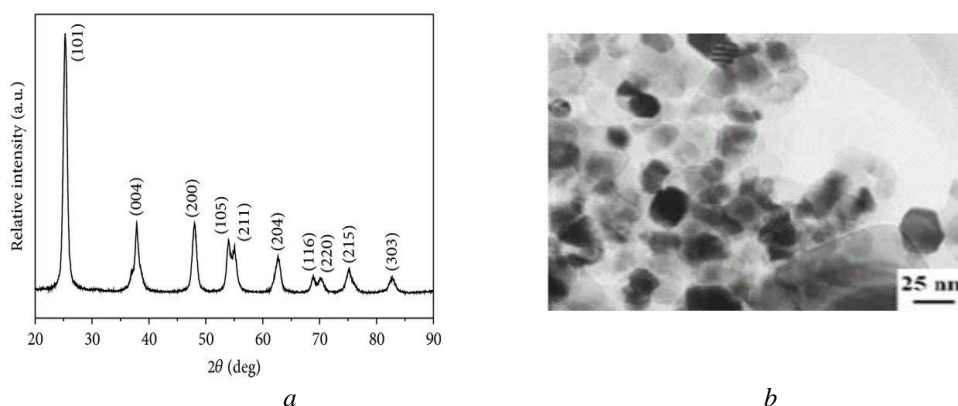


Fig. 3. XRD diffraction of the crystal structure of synthesized  $\text{TiO}_2$ -NPs powder in anatase phase (a). TEM bright field image of  $\text{TiO}_2$ -NPs (b). XRD, X-ray diffraction;  $\text{TiO}_2$ -NPs, titanium oxide nanoparticles; TEM, transmission electron microscopy.

### 3.3 Modeling and simulation results of nanofilter

The Table 1 compared filter mass flow rate, area-weighted average of pressure and velocity cantors in different between the inlet and outlet fluid of the nanofilter. The difference between the inlet and outlet fluid of nanofilter were increased for cantors of mass flow rate and area-weighted average of velocity levels (1.07 (g/s) and 0.289 (m/s), respectively). Remarkably, the net of pressure cantors had highest differences level ( $\leq 200$ -fold difference in the inlet and outlet fluid different).

Table 1. The comparative results of filter mass flow rate, area-weighted average of pressure and velocity cantors, accordance of Darcy equation.

	Inlet	Outlet	Net
Mass flow rate (g/s)	13.105	14.11	+ 1.07
Pressure (KPa)	2.941	413.215	+ 383.805
Velocity (m/s)	0.198	0.487	+0.289

Abbreviations: g/s, germ per second; KPa, kilopascal; m/s, meter per second.

The pressure and velocity cantors measured an area-weighted average of nanofilter.

The net value calculated from difference between the inlet and outlet fluid of nanofilter.

Due to the significant increase in the area-weighted average of pressure contour, all three cantors stimulated by CFD. Then, the results of Darcy equation, CFD, and experimental were compared for mass flow rate, area-weighted average of pressure cantors. This results showed Darcy equation is further simulation trends by increasing the porous medium flora. The results of comparison showed that CFD analysis is more accurate than Darcy predicted. This increased accuracy was associated with growing the porous medium flora of nanofilter. In Fig. 4, the porous medium has been compared between Darcy equation, CFD, and experimental results for outlet fluid of nanofilter. As seen in the Fig. 4, the Darcy equation, CFD, and experimental results for outlet fluid of nanofilter were similar with regard to area-weighted average of pressure and mass flow rate contours.

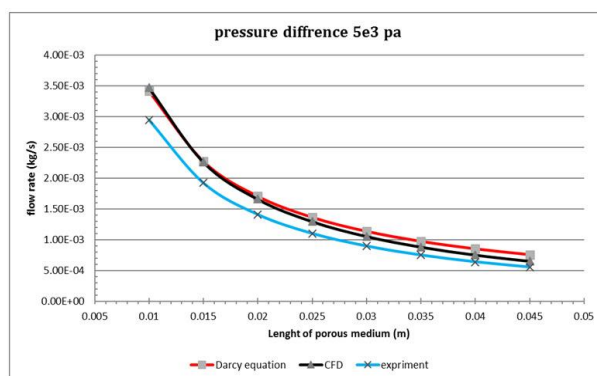


Fig. 4. The comparison of Darcy equation, CFD, and experimental results for outlet fluid of nanofilter. CFD, computational fluid dynamics.

### 3.4 Bactericidal effect of nanofilter

To evaluate the performance of the deigned nanofilter, 5 ml of combination soup were injected to systems. The combination soup defined the 1 ml of each studied bacterial species. As a Table 2 results, average initial injection of *E. coli* was  $203 \pm 146$  CFU/ml that after the filtering, closely 89.6% ( $181 \pm 21$  CFU/ml) of the prototype injection was filtered. Most of the filtering capability was for *S. dysenteriae* strain (90.1%;  $211 \pm 14$  CFU/ml from  $234 \pm 156$  CFU/ml of injected sample). In return, sporicidal capability of deigned nanofilter was the lowest in compared to other samples (80.8%;  $148 \pm 31$  CFU/ml from  $183 \pm 101$  CFU/ml of injected sample). Total coliform removal of nanofilter was  $44 \pm 27$  CFU/ml, through 85.8% of filtering capability.

Table 2. The comparison of bactericidal effect and filtering capability of nanofilter for each sample.

Strains	<i>E. coli</i>	<i>V. cholera</i>	<i>S. dysenteriae</i>	Spore of <i>C. botulinum</i>	Total coliform
Injected sample (CFU/ml)	$203 \pm 146$	$296 \pm 149$	$234 \pm 156$	$183 \pm 101$	$310 \pm 211$
Average removed (CFU/ml)	$21 \pm 14$	$31 \pm 17$	$23 \pm 14$	$35 \pm 21$	$44 \pm 27$
Filtering capability (%)	89.6	89.5	90.1	80.8	85.8

Abbreviations: CFU/ml, colony-forming unit (CFU) in milliliters; *E. coli*, *Escherichia coli*; *V. cholera*, *Vibrio cholera*; *S. dysenteriae*, *Shigella dysenteriae*; *C. botulinum*, *Clostridium botulinum*; SD, standard deviation.

All values were shown as the mean  $\pm$  SD of the mean of individual samples.

Total coliforms contains 10 ml of each of the studied strains.

Also, filtering capacity of nanofilter was compared in three consecutive filtration in the Fig. 5 for all investigated strains. In this test, three consecutive filtrations were repeated three times on 3 different days (with an interval of 24 h). As seen, the nanofilter capacity has been declining for 3<sup>th</sup> filtering in compared with 1<sup>th</sup> and 2<sup>th</sup> time of filtration. Statistically, a noteworthy

reduction of 3<sup>th</sup> filtering was established in *E. coli* (P=0.032), *S. dysenteriae* (P=0.0012) and spore of *C. botulinum* (P=0.048) samples in compared with 1<sup>th</sup> time of filtration (all P<0.005). Remarkably, a significant differences were observed between 3<sup>th</sup> and 2<sup>th</sup> filtering of *S. dysenteriae* (P<0.05), which its shown *S. dysenteriae* is easier to separations than other strains. More importantly, no significant differences was found for total coliform filtrations between three consecutive filtration (P=0.367).

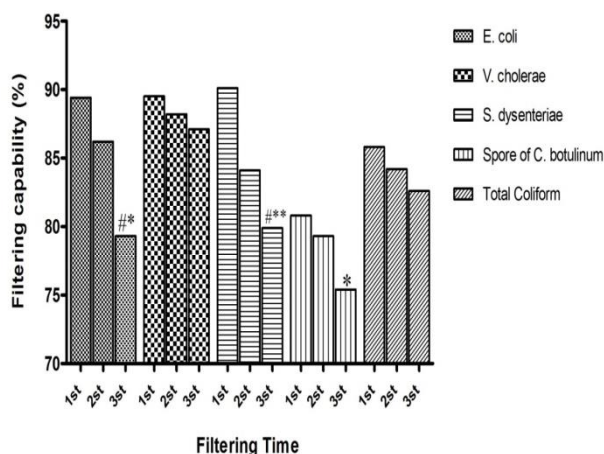


Fig. 5. Filtering capacity of nanofilter in three consecutive filtrations for all investigated strain. *E. coli*, *Escherichia coli*; *V. cholera*, *Vibrio cholera*; *S. dysenteriae*, *Shigella dysenteriae*; *C. botulinum*, *Clostridium botulinum*. Total coliforms contains 10 ml of each of the studied strains. \*: P<0.05 and \*\*: P<0.001 vs the 1<sup>th</sup> filtration. #: P<0.05 and ###: P<0.001 vs the 2<sup>th</sup> filtration.

A sample relationship between filtration capability of nanofilter correlated with time are shown in Fig. 6. This figure shown a significant negatively correlations between filtration capability and increasing of filtering time for removal of *E. coli* (R=-0.6, P=0.073, Fig. 6A), *V. cholera* (R=-0.87, P=0.041, Fig. 6B), and *S. dysenteriae* (R=-0.95, P=0.032, Fig. 6C). Conversely, the removal capability of nonfilter for Spore of *C. botulinum* and total coliform was positive correlated to increasing of filtering time (R=0.846, P=0.12; R=0.81, P=0.93, respectively) (Fig. 6 D&E).

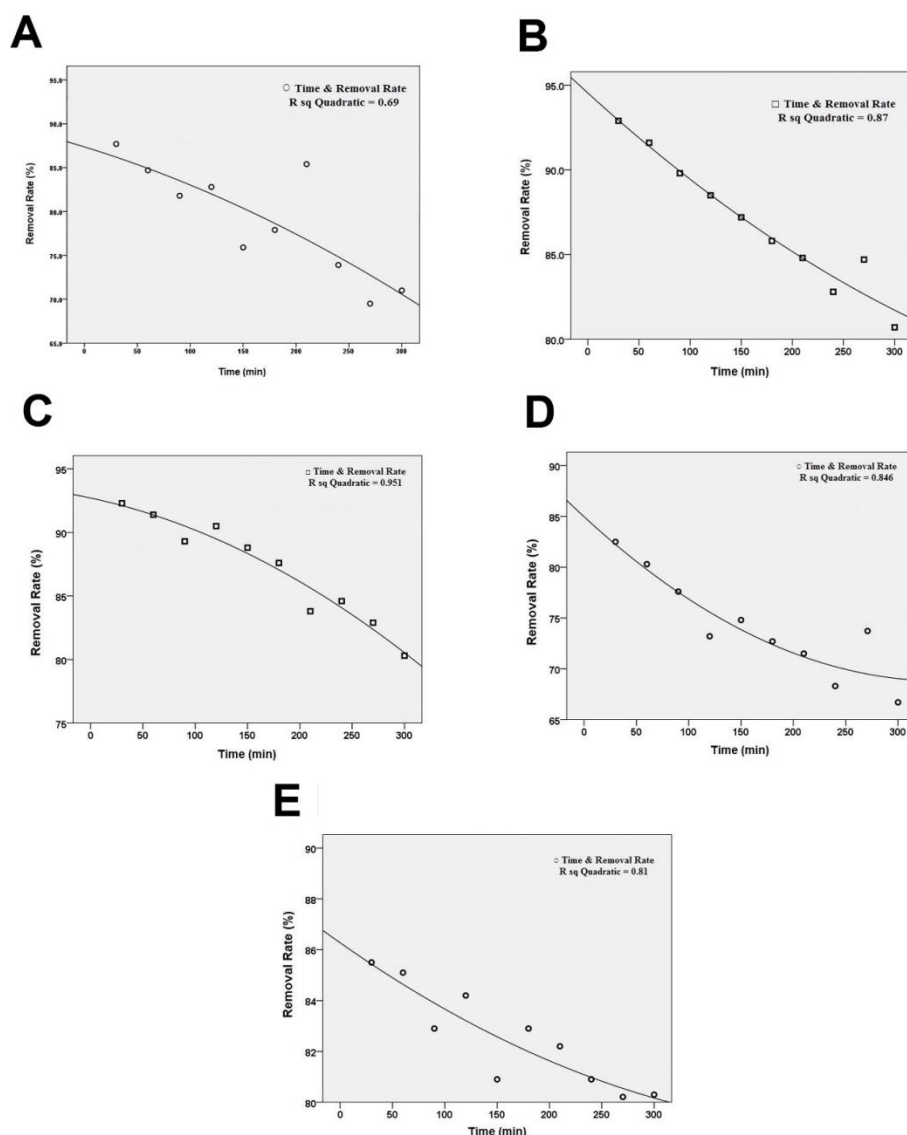


Fig. 6. Proportions of filtration capability of nanofilter correlated with filtering time. This figure shown the negative correlation between removal capability of nonfilter for *E. coli* (a), *V. cholera* (b), and *S. dysenteriae* (c) by filtering time, in front of positive correlations between the removal capability of nonfilter for Spore of *C. botulinum* (d) and total coliform (e) with time. The line is the regression line calculated with SPSS (Chicago, Illinois, USA) and spearman's rank correlation coefficient ( $r$ ). *E. coli*, *Escherichia coli*; *V. cholera*, *Vibrio cholera*; *S. dysenteriae*, *Shigella dysenteriae*; *C. botulinum*, *Clostridium botulinum*; Total coliforms contains 10 ml of each studied strains.

#### 4. Discussion

In this report, we presented the first detailed novel diatomaceous photo catalysis-assisted water filter that design based photocatalytic properties of  $\text{TiO}_2$ -NPs on the frustule nanostructures. According our mind, the diatoms played roles both bio templates and resources of Si in the synthetic nanofilter. These findings indicated significant increase of the filtrations capacity of diatomaceous nanostructures- based filter compared to combination diatomaceous filter with  $\text{TiO}_2$ -NPs. Our results highlighted that the combination of the diatom structure and the existence of the  $\text{TiO}_2$ -NPs in the as-prepared  $\text{TiO}_2$ -NPs/ $\text{SiO}_2$  composite render it as improved photocatalytic performance under UV-light irradiation. Also, synthetic  $\text{TiO}_2$ -NPs were in the range size of 20-40 nm. To the best of our knowledge, anatase phase of  $\text{TiO}_2$ -NPs have the most catalytic properties.

Recent studies have proved that SiO<sub>2</sub> in the diatomaceous nanostructures can also narrow down the band gap of TiO<sub>2</sub>-NPs leading to its excitation in the visible region. However TiO<sub>2</sub>-NPs on photo-irradiation by fluorescent light can be excited leading to the generation of electrons and holes (Gordon et al., 2009). These excited electrons can then drift in to the conduction and of SiO<sub>2</sub> in the diatomaceous nanostructures since its work function is higher than TiO<sub>2</sub>-NPs (Oza et al., 2013, Li et al., 2015a). Even though incorporation of silica, it did not provide a high surface area for adsorption and reaction sites, the TiO<sub>2</sub>-NPs/SiO<sub>2</sub> deigned its morphology from diatoms due to well-maintained silica frustules which are closely the significant of advantage the UV-harvesting of frustules nanostructures (Eike Brunner et al., 2009). Morphologically, the frustules nanostructures in diatomaceous maintained the hierarchical structures of TiO<sub>2</sub>-NPs/SiO<sub>2</sub> in the deigned nanofilter. Meanwhile, like diatom cells, the frustules, can control the propagation of UV, so the photo-generated electrons channeling and focusing properties of their SiO<sub>2</sub> structure could help the transmissions and collection of more photo-generated electrons into the bacterial or microbial cell surface (Jiao He et al., 2013). Also, there is evidence to suggest that UV-sensitive TiO<sub>2</sub>-NPs coatings enhanced the light-harvesting ability as well as improved the photocatalytic activity of nanofilter (Gordon et al., 2009, T. Fuhrmann et al., 2004).

It is hypothesized that the photo-generated electrons in SiO<sub>2</sub> of diatomaceous nanostructures might react with the dissolved oxygen molecules, thus generating oxygen peroxide radicals (O<sub>2</sub><sup>•-</sup>). Holes created in TiO<sub>2</sub>-NPs may react with the OH<sup>-</sup> which is obtained from water molecules to form hydroxyl radicals (OH•). Then all microbial stains can be photo catalytically killed by both OH• and O<sub>2</sub><sup>•-</sup> (X. Zhang et al., 2011, D. Robert, 2007, Field et al., 1998).

The most important finding of this study lies in sporicidal capability of deigned nanofilter was the lowest in compared to other samples (80.8%; 148±31 CFU/ml from 183±101 CFU/ml of injected sample). In return, total coliform removal of nanofilter were 85.8% of filtering capability. Importantly, the filtering capability was for *S. dysenteriae* strains (90.1%; 211±14 CFU/ml from 234±156 CFU/ml of injected sample). Our investigations showed that the nanofilter capacity has been declining for 3<sup>th</sup> filtering in compared with 1<sup>th</sup> and 2<sup>th</sup> time of filtration. Curiously, a significant differences were observed between 3<sup>th</sup> and 2<sup>th</sup> filtering of *S. dysenteriae* (P<0.05), which presented *S. dysenteriae* is easier to filtrations than other strains. More notably, no significant differences was initiate for total coliform filtrations between three consecutive filtration (P=0.367). It is quite clear that gram-negative bacteria such as *S. dysenteriae* are weaker and more favorable for filtering in front of disinfectants and cleaners against, probably due to the structure of the cell walls and accumulation of negative charges of lipopolysaccharides (LPS), the major component of the outer membrane of gram-negative bacteria (Lam et al., 2014, Gilbert et al., 1990).

Finally, the current study was limited by variables such as the size and composition of the nanofilter. The present study has only investigated the 10% (v/v) of TiO<sub>2</sub>-NPs and diatomaceous soil. Also simulated this composition in the 30 mm cylindrical model of nanofilter (30×100 mm), which admittedly for different sizes and composition can be obtained the better and more debatable results. Our investigations into this area are still ongoing to accesses the NPs-based filtering diatoms structure.

## 5. Conclusion

In summary, we stimulated and deigned scalable paraphernalia, TiO<sub>2</sub>-NPs/SiO<sub>2</sub> composite, for the removal of main coliform from water. The SiO<sub>2</sub> of diatomaceous nanostructures can be used as a template to augment the photocatalytic specific surface area as well as increase apparent quantum efficiency owing to their high aspect ratio and unique electrical properties. Since it has got metallic properties, TiO<sub>2</sub>-NPs can act as a sink for photo induced charge transferors stimulating interfacial charge transmission processes. So, frustule nanostructures TiO<sub>2</sub>-treated is appropriate for filtering of water coliforms.

## Acknowledgments

This research was supported partially by the Iran national Science foundation, Science deputy of Presidency, the Research Foundation of the Science and Technology Department of Sichuan Province (14JC0797, 2015JY0038), and Southwest Medical University Grant for Postdoctoral Research. The authors thank people who provided samples.

## Reference

- [1] Ali Mohammad Zand, Saber Imani, Mojtaba Saadati, Hossein Honari, Saeed Rezaei-Zarchi, Amene Javid, Mokhtare Zareh & Doroudian, M. *African Journal of Microbiology Research* **6**, 1417 (2012).
- [2] S. Baron, I. Kaufmann Alves, T. G. Schmitt, S. Schoffel, J. Schwank, *Water Sci Technol*, **72**, 1730 (2015).
- [3] M. R. Bilad, V. Discart, D. Vandamme, I. Foubert, K. Muylaert, I. F. Vankelecom, *Bioresour Technol*, **138**, 329 (2013).
- [4] S., Chandrasekaran, T. J. Macdonald, A. R. Gerson, T. Nann, N. H. Voelcker, *ACS Appl Mater Interfaces*, **7**, 17381 (2015).
- [5] D. Robert. *Catal. Today*, **122**, 20 (2007)
- [6] B. Delalat, V. C. Sheppard, S. Rasi Ghaemi, S. Rao, C. A. Prestidge, Mcphee, G., Rogers, M. L., Donoghue, J. F., Pillay, V., Johns, T. G., Kroger, N. & Voelcker, N. H. *Nat Commun*, **6**, 8791 (2015)
- [7] Eike Brunner, Patrick Richthammer, Hermann Ehrlich, Silvia Paasch, Paul Simon, Ueberlein S., Van, K.-H.. *Angewandte Chemie International Edition*, **48**, 9724 (2009).
- [8] C. B. Field, M. J. Behrenfeld, J. T. Randerson, P. Falkowski, *Science*, **281**, 237 (1998)
- [9] M. FUNAYAMA, Y. AOKI, I. M. SEBETAN, K. SAGISAKA, *Forensic Sci Int*, **34**, 175 (1987).
- [10] G. Gao, Q. Zhang, Z. Hao, C. D. Vecitis, *Environ Sci Technol*, **49**, 2375 (2015).
- [11] P. Gilbert, D. Pemberton, D. E. Wilkinson, *J Appl Bacteriol*, **69**, 593 (1990)
- [12] R. Gordon, D. Losic, M. A. Tiffany, S. S. Nagy, F. A. Sterrenburg, *Trends Biotechnol*, **27**, 116 (2009)
- [13] Jiao He, Daomei Chen, Yongli Li, Junlong Shao, Jiao Xie, Yuejuan Sun, Zhiying Yan & Wang, J. *Applied Physics A*, **113**, 327 (2013)
- [14] J. Keeley, P. Jarvis, A. D. Smith, S. J. Judd, *Coagulant recovery and reuse for drinking water treatment. Water Res*, **88**, 502 (2016).
- [15] M. M., Khan, V., Filiz, G., Bengtson, S., Shishatskiy, M. Rahman, V. Abetz, *Nanoscale Res Lett*, **9**, 2421 (2014).
- [16] K., Kim, E., Seo, S. K., Chang, T. J. Park, S. J. Lee, *Sci Rep*, **6**, 20426 (2016).
- [17] J. S., Lam, E. M. Anderson, Y. Hao, *Methods Mol Biol*, **1149**, 375 (2014).
- [18] J., Li, T., Liu, G. Sui, D. Zhen, *J Nanosci Nanotechnol*, **15**, 1408 (2015a).
- [19] Y., Li, L., Cao, L. Li, C. Yang, *J Hazard Mater*, **289**, 140 (2015b)
- [20] Z., Li, C., Yao, F., Wang, Z. Cai, X. Wang, *Nanotechnology*, **25**, 504005 (2014).
- [21] Y., Liu, H., Liu, Z., Zhou, T., Wang, C. N. Ong, C. D. Vecitis, *Environ Sci Technol*, **49**, 7974 (2015).
- [22] G. K., Mor, K., Shankar, M., Paulose, O. K. Varghese, C. A. Grimes, *Nano Lett*, **5**, 191 (2005).
- [23] G., Oza, S., Pandey, A., Gupta, S., Shinde, A., Mewada, P., Jagadale, M. Sharon, M. Sharon, *Mater Sci Eng C Mater Biol Appl*, **33**, 4392 (2013).
- [24] PAI. 1997. *Sustaining Water, Easing Scarcity: A Second Update*. Revised data for the population action international report, sustaining water: Population and the future of renewable water supplies [Online]. water97.
- [25] M., Sakai, M. Kawakami, K. Amada, *J Environ Sci (China)*, **25** Suppl 1, S132 (2013)
- [26] R. P., Scherer, C. M., Sjunneskog, N. R. Iverson, T. S. Hooyer, *J Nanosci Nanotechnol*,

- 5**, 96 (2005).
- [27] T. Fuhrmann, S. Landwehr, M. El Rharbi-Kucki, M. Sumper, *Applied Physics B*, **78**, 257 (2004)
- [28] M. Thakkar, Z. Wu, L. Wei, S. Mitra, *J Colloid Interface Sci*, **450**, 239 (2015)
- [29] G. Wang, Q. Wang, W. Lu, J. Li, *J Phys Chem B*, **110**, 22029 (2006).
- [30] Y. Wang, J. Pan, J. Cai, D. Zhang, *FBiochem Biophys Res Commun*, **420**, 1 (2012)
- [31] X. Zhang, X. Zhao & H. Su, *Korean J. Chem. Eng.*, **28**, 1241 (2011)
- [32] S. Zhang, D. Jiang, H. Zhao, *Environ Sci Technol*, **40**, 2363 (2006).